2018

Estimating passive stress acting on a grain entrapment victim's chest

Salah F. Issa
Purdue University

Carl Wassgren
Purdue University

Charles V. Schwab
Iowa State University, cvschwab@iastate.edu

Richard Stroshine
Purdue University

William E. Field
Purdue University

Estimating passive stress acting on a grain entrapment victim's chest

Abstract

Grain entrapments remain a major concern in the grain industry, with 1,100 incidents documented since the 1970s. One particular concern is the ability of a victim to breathe while entrapped in grain. Anecdotal reports suggest that victims struggle to breathe when entrapped in grain to a depth that covers their chests, yet some evidence indicates that victims should be able to breathe normally as long as their airways are not blocked regardless of depth. The hypothesis for this discrepancy is that previously published experiments measured an active stress state in the grain, while a person breathing also experiences a passive stress state during inhalation. The passive stress is significantly larger than the active stress. The objective of this study was to measure the passive stress when pushing against grain, such as during inhalation, and compare it to active stress state measurements. An MTS Criterion testing machine, which is a force deformation testing device, was used to push a block horizontally against a column of grain and record the force and displacement during the movement. The measured passive stress was calculated from the force and displacement values and ranged from 9.4 to 11.0 kPa at a depth of 20 to 30 cm. These values are three to four times larger than previously published measurements of stresses at similar depths. This result indicates that the discrepancy between experimental results and anecdotal reports is most likely due to the type of stress state experienced in grain entrapment. Findings imply that the pressures on the victim's chest during entrapment are sufficient to cause breathing difficulties or crush/positional asphyxiation in some cases. A full-scale study is recommended.

Keywords

Active pressure, Corn pressure, Farm safety, Grain rescue, Passive pressure, Rib cage

Disciplines

Agriculture | Bioresource and Agricultural Engineering | Ergonomics

Comments

This article is published as Issa, Salah F., Carl Wassgren, Charles V. Schwab, Richard Stroshine, and William E. Field. "Estimating Passive Stress Acting on a Grain Entrapment Victim's Chest." *Journal of Agricultural Safety and Health* 24, no. 3 (2018): 113-126. DOI: 10.13031/jash.12552. Posted with permission.

Estimating Passive Stress Acting on a Grain Entrapment Victim's Chest

S. F. Issa, C. Wassgren, C. V. Schwab,
R. Stroshine, W. E. Field

ABSTRACT. *Grain entrapments remain a major concern in the grain industry, with 1,100 incidents documented since the 1970s. One particular concern is the ability of a victim to breathe while entrapped in grain. Anecdotal reports suggest that victims struggle to breathe when entrapped in grain to a depth that covers their chests, yet some evidence indicates that victims should be able to breathe normally as long as their airways are not blocked regardless of depth. The hypothesis for this discrepancy is that previously published experiments measured an active stress state in the grain, while a person breathing also experiences a passive stress state during inhalation. The passive stress is significantly larger than the active stress. The objective of this study was to measure the passive stress when pushing against grain, such as during inhalation, and compare it to active stress state measurements. An MTS Criterion testing machine, which is a force deformation testing device, was used to push a block horizontally against a column of grain and record the force and displacement during the movement. The measured passive stress was calculated from the force and displacement values and ranged from 9.4 to 11.0 kPa at a depth of 20 to 30 cm. These values are three to four times larger than previously published measurements of stresses at similar depths. This result indicates that the discrepancy between experimental results and anecdotal reports is most likely due to the type of stress state experienced in grain entrapment. Findings imply that the pressures on the victim's chest during entrapment are sufficient to cause breathing difficulties or crush/positional asphyxiation in some cases. A full-scale study is recommended.*

Keywords. *Active pressure, Corn pressure, Farm safety, Grain rescue, Passive pressure, Rib cage.*

Grain entrapments remain a topic of interest in the scientific and safety communities, with 1,172 incidents documented by the Purdue Agricultural Safety and Health Program (Issa et al., 2017a). There has been significant research on the amount of force required to pull an entrapped body out of a grain mass and the body's ability to withstand extrication forces (Schmechta and Matz, 1971; Schwab et al., 1985; Roberts et al., 2015; Issa and Field, 2017). However, research on the pressures that a victim experiences while buried in a grain

Submitted for review in July 2017 as manuscript number JASH 12552; approved for publication by the Ergonomics, Safety, & Health Community of ASABE in May 2018.

The authors are **Salah F. Issa,** Post-Doctoral Research Associate, Department of Agricultural Biological Engineering, and **Carl Wassgren,** Professor, School of Mechanical Engineering, Purdue University, West Lafayette, Indiana; **Charles V. Schwab,** Professor, Department of Agricultural and Biosystems Engineering, Iowa State University, Ames, Iowa; **Richard Stroshine,** Professor, and **William E. Field,** Professor, Department of Agricultural Biological Engineering, Purdue University, West Lafayette, Indiana. **Corresponding author:** Salah Issa, 225 S. University St., West Lafayette, IN 47907; phone: 201-618-0482; e-mail: salahfuadissa@gmail.com.

mass remains limited. Moore and Jones (2017) placed particular emphasis on the chest region, conducting the only known experiment in which the horizontal pressures on the chest and torso of a mannequin submerged in shelled corn were measured using a sensor mat. Moore and Jones (2017) found that the pressures exerted on the mat were 2.8 kPa at a 0.23 m depth and 3.9 kPa at a 1.12 m depth; they concluded that the pressure the victim experiences was not significant enough to cause crush asphyxiation. However, these results appear contradictory to grain entrapment data, in which 7% of all entrapment cases (with the head visible) resulted in a fatality (Issa et al., 2017b). In addition, from anecdotal data, many of the survivors of grain entrapments found breathing difficult even in shallow entrapments. The aim of this study was to reconcile the differences between existing experimental results and anecdotal reports.

Active versus Passive Stress States

To understand the forces that the chest and torso experience, it is important to understand how stresses vary within grain. The first comparative example to look at is Newtonian fluids such as water. In such fluids, the (gauge) pressure P is given by $P = \rho g h$, where ρ is the fluid density, g is the gravitational acceleration, and h is depth from the free surface. This pressure acts equally in all directions and is independent of the diameter of the container. In cereal grains, the vertical (σ_V) and horizontal (σ_H) stresses are not equal but are instead related by the material's Janssen constant, k (refer to Nedderman, 1992, for additional details):

$$\sigma_H = k\sigma_V \tag{1}$$

The exact value of the constant in the Janssen equation depends on the boundary conditions, but two limiting values can be defined depending on the effective internal friction angle of the grain (δ):

$$k_{A/P} = [1 -/+ \sin(\delta)]/[1 +/- \sin(\delta)]. \tag{2}$$

The choice of plus or minus symbols in equation 2 depends on whether the material is in an active (A) or passive (P) stress state. In an active stress state, the horizontal stress is smaller than the vertical stress, and the first symbols should be used, i.e., $k_A = [1 - \sin(\delta)]/[1 + \sin(\delta)] < 0$. In a passive stress state, the horizontal stress is larger than the vertical stress, and the second symbols should be used, i.e., $k_P = [1 + \sin(\delta)]/[1 - \sin(\delta)] > 0$. The difference in the Janssen constant for the two stress states can be substantial. For example, the effective internal friction angle for cereal grains at safe storage moistures is in the range of 16° to 30° (Bhadra et al., 2017); for an angle of 20°, $k_A = 0.5$ and $k_P = 2.0$. Thus, the horizontal stress can vary by nearly an order of magnitude and in this case by a factor of 4.

Two examples can be used to illustrate the two types of stresses that can occur in a bin filled with grain. An active stress state develops if the walls of the bin expand outward, allowing the grain to settle vertically. Similarly, the stress state is passive if the walls of the bin are pushed inward so that the grain is pushed upward. These limiting stress states are useful in explaining the stresses experienced by a person entrapped in grain. During exhalation, the grain near the victim's chest is in an active state as the chest cavity shrinks. The horizontal stress pressing against the chest is smaller than the vertical stress for this case. However, when the person inhales and the chest cavity expands, the surrounding grain is in a passive state, and the horizontal stress acting on the chest is larger than the vertical stress. Thus, the work required to inhale can be substantial.

This analysis helps explain the difference between previously published experimental results and anecdotal reports of grain entrapments. It is proposed that the experiment conducted by Moore and Jones (2017) measured an active stress, which is the stress state that typically occurs during filling of a vertical-walled bin, an example used by Nedderman (1992). However, the chest of a living entrapped victim is expanding and contracting due to breathing and thus experiences alternating active stresses during exhalation and passive stresses during inhalation as the chest expands and pushes against the grain. Therefore, a live victim entrapped in grain experiences a substantially larger force than what is measured by load cells attached to a non-breathing mannequin.

The objective of this study was to measure the potential stresses acting on the chest of someone entrapped in shelled corn, to confirm that the entrapped victim's chest experiences passive stresses when the victim attempts to breath, and to confirm that this passive stress is larger than the active pressure measured by static load cells. Throughout this article, the term stress refers to the scientific definition of stress and not the mental or physical state of a grain entrapment victim. Pressure refers to the average of normal stresses and thus is not the correct term to describe passive and active stresses in this article. However, when citing work that uses the term pressure, that term is used for consistency when describing the published values.

Methods

To measure passive stress, a three-celled box was built to push grain using a pair of wooden blocks. A welded steel box measuring 40.6 cm × 40.6 cm (16 in. × 16 in.) and 46.0 cm (18.1 in.) tall was built (fig. 1). An 8.3 cm wide × 5.7 cm high (3.25 in. × 2.25 in.) rectangular hole was cut into each of two steel panels, which were both 40.6 cm wide and 46.0 cm high (16 in. × 18.1 in.). The rectangular holes were located 10.2 cm from the

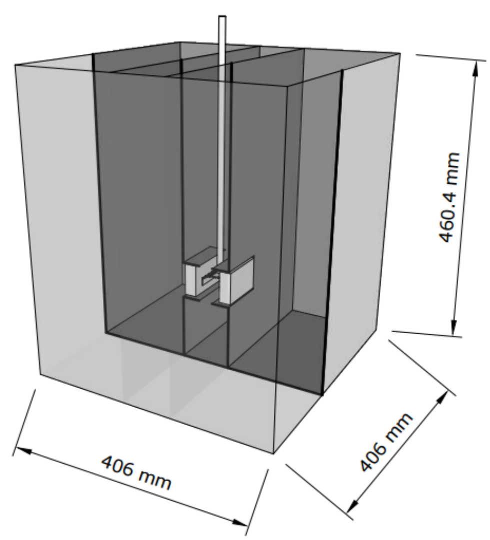

Figure 1. Welded box designed to measure passive grain pressure. The rod is attached to a load cell on a Criterion testing machine (not shown). As the Criterion machine pushes the rod downward, the hinges push the blocks horizontally.

bottom edges of the panels and centered horizontally (fig. 2). The holes were created by cutting slits across the center and along sides of the holes and then bending the steel to create two shelves to hold the wooden blocks in place (figs. 1 and 2b). The panels were then placed in the box to create three cells (figs. 1 and 2). The two outer cells were each 15.6 cm (6.1 in) wide.

The rectangular holes allowed two 7.6 cm × 5.1 cm (3 in. × 2 in.) wooden blocks to pass through them and press on the grain that was placed in the two outer cells (fig. 2a). The blocks were made of oak, and their sides were sanded and sprayed with 3-in-One Lock Dry Lube (3-in-One, Budd Lake, N.J.) to reduce friction between the blocks and the steel shelves. The blocks were attached by hinges to a 40.6 cm (16 in.) rod. Forces exerted on the blocks were transferred through the hinges and rod to a 500 N load cell (model LPB.502, 2.328 mV/V sensitivity) that was in turn attached to the crosshead on the load frame of a Criterion testing machine (model 43, MTS Systems Corp., Eden Prairie, Minn.).

The two outer cells (fig. 1) were filled with corn to within several millimeters of the top and leveled using a small wooden spatula. The Criterion machine was programmed to lower the crosshead (with the attached rod) 18 mm vertically at a rate of 0.1 mm s^{-1}. This displacement corresponded to pushing the blocks into the grain approximately 5.1 mm, with a standard deviation (SD) of 0.9 mm. This movement created a passive stress state within the grain, similar to what would be experienced by an expanding chest cavity during inhalation.

In addition to the 30.5 cm (12 in.) grain depth, data were collected for depths of 20.3 cm (8 in.) and 10.2 cm (4 in.). The depths were chosen to reflect a person entrapped in grain approximately to the mouth/nose level. Six replicates were conducted at each grain depth. An experiment was also conducted with no grain in the cells to measure the frictional forces exerted on the blocks as they moved through the rectangular holes. Three replicates with no grain in the cells were conducted, and the load cell recorded a maximum force of 0.9 to

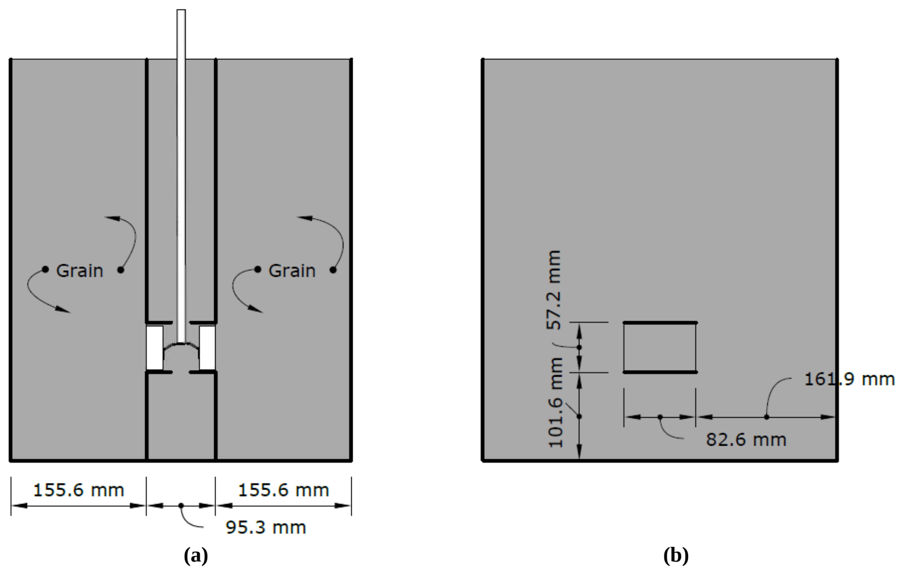

Figure 2. (a) Cross-section of the welded box showing how the blocks are connected to the rod and how they push the grain and (b) one of the interior panels showing the location of the rectangular hole.

2.8 N in each replicate. At the end of the study, a run with no grain was conducted to ensure that the lubrication on the blocks was not removed during the experiments. The maximum force recorded in that final run was 1.3 N, while the maximum force ranged from 25 to 47 N with grain in the cells (depending on the depth of grain).

Friction Test

To gain a better understanding of what the load cell was measuring, a simpler experiment was designed in which values of the friction coefficient of steel on steel were measured. In this simpler experiment, the only unknown is the friction coefficient. Thus, the friction coefficient can be calculated using a standard force equation and the force reported by the load cell and confirm what the load cell is measuring. In addition, values of the friction coefficient are available in the literature and could be compared to a control experiment. The rod with the wooden blocks was placed on a flat steel surface. Four steel weights of approximately 418 g each were placed on either side of the blocks (two on each side). The Criterion machine was then programmed to move the rod downward at a prescribed rate. This pushed the blocks and weights outward. Because the only force resisting the movement of the blocks was the friction force between the weights and the steel plate, the load cell values could be used to calculate the friction coefficient of steel on steel. As in the experiments with corn, the wooden blocks were lubricated with 3-in-One Lock Dry Lube.

Using only the blocks (no steel weights), the load cell recorded a maximum force of 0.3 N per replicate. The load cell used in the friction experiment was a 50 N load cell (model LSB.501, 1.972 mV/V sensitivity) due to the lower force values (3 to 5 N) anticipated. The crosshead of the Criterion machine was lowered vertically at a rate of 0.1 mm s^{-1}. The experiment was also conducted at rates of 1 and 0.01 mm s^{-1}, and no significant differences were observed between each of the three rates (fig. 3). The 0.1 mm s^{-1} crosshead speed was chosen because it provided about 2000 data points. In addition, as a control, the force required to pull the steel blocks across the same steel surface was measured to get an independent measurement of the friction coefficient of steel on steel (Issa, 2016). Each test was repeated five times.

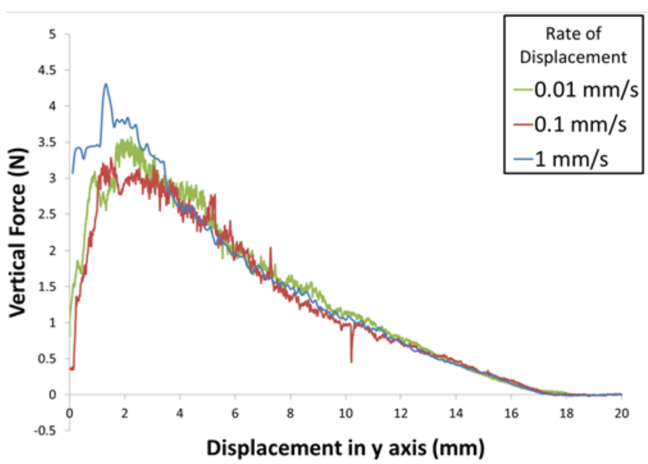

Figure 3. Comparison of different displacement rates for measurement of the friction coefficient of steel.

Virtual Work Calculations

To determine the forces acting on a wooden block in both the actual experiments and the friction test, an energy balance method using the principle of virtual work and a free-body diagram (fig. 4) were used:

$$\delta W = 0 = F\delta y + 2W\tfrac{1}{2}\delta y - 2R\delta x - 2f\delta x \tag{3}$$

where F and P are the vertical and horizontal pin forces, respectively, applied by the Criterion machine on the bar, W is the weight of the hinge side plate, R is the force the grain exerts on the wooden block, which is in turn exerted on the bar, n is the normal force exerted on the bar by the guide shelf (shown in fig. 2), f is the frictional force acting on the bar due to the guide shelf, θ is the angle the bar makes with the horizontal, and δy and δx are the virtual displacements in the vertical and horizontal directions, respectively. Note that due to symmetry, the bar weight, reaction, and friction forces are doubled in equation 3. The hinge does not move in the x direction at the point where P is acting, and it does not move in the y direction at the point where n is acting. Because these forces do not move through a distance, they do not contribute to the virtual work and are not included in equation 3. Solving for R gives:

$$R = \left(F + W\right)\frac{\delta y}{2\delta x} - f \tag{4}$$

From the geometry in figure 4b and the Pythagorean theorem, we obtain the following relationship between δy and δx:

$$\delta x = \delta y \tan\theta \quad \text{where} \quad \tan\theta = \frac{y}{\sqrt{L^2 - y^2}} \tag{5}$$

Substituting equation 5 into equation 4 gives:

$$R = \left(F + W\right)\frac{\sqrt{L^2 - y^2}}{2y} - f \tag{6}$$

The force F is assumed to be zero when there is no bar attached to the load cell measuring this force. Because the load cell was tared after insertion of the rod but before adding grain, the measured/tared force F' is defined as:

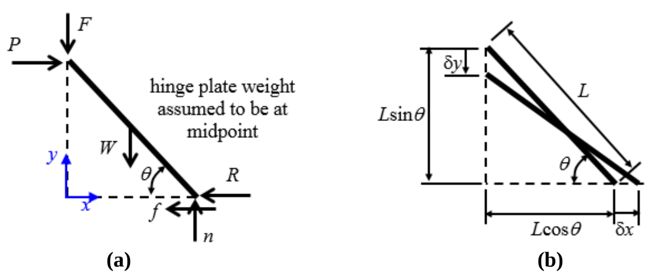

Figure 4. Free-body diagrams of one of the two hinge side plates showing the forces applied by the rod and wooden block.

$$F' \equiv F - F_{y_0} = F - \left[\frac{2y_0}{\sqrt{L^2 - y_0^2}} \left(R_{y_0} + f_{y_0} \right) - W \right] \tag{7}$$

where y_0 is the vertical location at which the load cell is tared. Thus, at position y_0, the tared load cell will register $F' = 0$ and $R_{y0} = 0$. The block force R can be found in terms of the tared force by substituting equation 7 into equation 6:

$$R = F' \frac{\sqrt{(L^2 - y^2)}}{2y} - f' \tag{8}$$

where f' is defined as:

$$f' \equiv f - \left[\frac{2y_0}{\sqrt{\left(L^2 - y_0^2\right)}} \times \frac{\sqrt{\left(L^2 - y^2\right)}}{2y} \right] \times f_{y_0} \tag{9}$$

For the complete derivation, refer to the Appendix.

The load cell output provided the applied vertical force, which was sampled every 0.1 s. Equation 8 can be used to calculate the force R for each sampled force. The average R is determined by taking an average of all values within a range that starts when the hinge has moved 5° after beginning the experiment and ends when the hinge is 5° from its value at the end of the experiment (fig. 5). The displacements in the x and y directions were calculated by fitting a cosine function to the force-displacement curve to predict the initial and subsequent angles of the hinge. The frictional component of the equation was determined by conducting the experiment without grain ($R = 0$). To calculate the passive stress, the average resultant force was divided by the surface area of the block in contact with the grain. For the experiment with steel weights, the friction coefficients were calculated by dividing the resultant force by the mass of the steel weights.

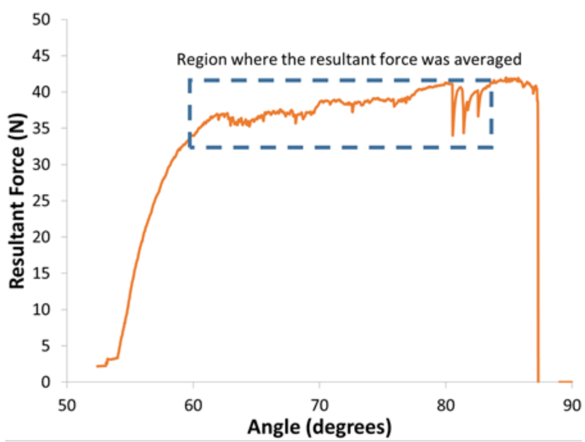

Figure 5. Sample force curve showing the region used to calculate the average force. The angle (θ) on the *x*-axis is defined in figure 4.

Uncertainty Analysis

The relative uncertainty in R (u_R, expressed as a percentage) due to measurement uncertainties in F', L, f', and y (eq. 9) was calculated as follows:

$$u_R = \sqrt{u_{R,F'}^2 + u_{R,L}^2 + u_{R,f'}^2 + u_{R,y}^2} \tag{10}$$

where

$$u_{R,F'} = \frac{1}{R}\frac{\partial R}{\partial F'}\delta F' = \frac{1}{R}\left[\frac{\sqrt{L^2 - y^2}}{2y}\right]\delta F' \tag{11}$$

$$u_{R,L} = \frac{1}{R}\frac{\partial R}{\partial L}\delta L = \frac{1}{R}\left[\left(F' + W\right)\frac{L}{2y\sqrt{L^2 - y^2}}\right]\delta L \tag{12}$$

$$u_{R,f'} = \frac{1}{R}\frac{\partial R}{\partial f'}\delta f' = \frac{1}{R}(-1)\delta f' \tag{13}$$

$$u_{R,y} = \frac{1}{R}\frac{\partial R}{\partial y}\delta y = \frac{1}{R}\ F' \times\left[\frac{-1}{2\sqrt{\left(L^2 - y^2\right)}} - \frac{\sqrt{\left(L^2 - y^2\right)}}{2y^2}\right]\delta y \tag{14}$$

and $\delta F'$, δL, $\delta f'$, and δy are the absolute uncertainties in F, W, L, f, and y, respectively. Uncertainty was calculated instantaneously, and the uncertainties in each parameter were measured as follows:

- $\delta F'$ and $\delta f'$ were measured by taking the standard deviation of a small interval (±0.5 s) around the point in question (±0.5 s).
- δL was based on the accuracy of the measuring device (δL = 0.05 mm).
- δy was the standard deviation of y between replicates (δy = 1.27 mm).

Statistical Analysis

In addition to uncertainty analysis, regression analysis and standard two-tail t-tests ($p < 0.05$) were run using Excel (Microsoft Corp., Redmond, Wash.) to explore the relationships and differences between replicate runs for the friction test and the passive stress test.

Grain Properties

Corn was selected for this experiment due to its prevalence in grain entrapments (Issa et al., 2016). The moisture content, bulk density, size, and angle of repose were measured (table 1). To obtain representative samples, the sample was poured through a Boerner divider (Seedburo Quality, Chicago, Ill.) several times, splitting the sample into two halves

Table 1. Grain properties for corn used in experiment.

Property	Value
Bulk density (ρ)	760.5 ±1.4 kg m^{-3}
Moisture content	13.7% ±0.1%
Dynamic angle of repose	20.4° ±0.4°
Major diameter (length)	12.1 ±1.4 mm
Intermediate diameter (width)	8.0 ±0.8 mm
Minor diameter (thickness)	4.8 ±0.9 mm

and then splitting one of the two halves again, until a sample weighing approximately 1 kg was obtained (Issa, 2016). Moisture content measurements were based on ASABE Standard S352.2 (ASABE, 2012). Bulk density was determined by filling a 1.1 L (one dry quart) cup using a funnel, leveling the surface, measuring the grain mass (in kg), and dividing the mass by 0.0011 m^3 to obtain the bulk density in kg m^{-3} (Clementson et al., 2010). Size was measured using a 15.24 cm (6 in.) Fowler Sulvac Model S 235 Data Caliper (Cole-Parmer Instrument Co., Vernon Hills, Ill.). The dynamic angle of repose for piling was measured by pouring a sample into a funnel, opening the funnel outlet so that the grain dropped onto a flat surface, and measuring the diameter and height of the grain pile. The grain (1.5 L, 1.34 kg) was dropped from a height of 8 cm onto a cardboard surface (Issa, 2016). This method is similar to the method reported by Ileleji and Zhao (2008) for angle of repose (loose base); the primary difference is the drop height (8 cm vs. 23 cm) due to the type of material (chopped biomass vs. corn).

Stress Calculations

While there are many methods for modeling the pressure in the system, due to the small size of the system, the hydrostatic method was used to estimate vertical stress, and equation 2 was used to estimate the active and passive stresses. To determine the forces on the wooden block as a whole, the hydrostatic equation was integrated with respect to height, resulting in the following equation:

$$\sigma_V = \rho g L\left(\frac{h_2^2}{2} - \frac{h_1^2}{2}\right) \tag{15}$$

where ρ is the bulk density of the grain (kg m^{-3}), g is the gravitational acceleration (m s^{-2}), L is the length of the block (m), and h_1 and h_2 (m) are the depth of the top and bottom of the block, respectively, from the surface of the grain. The measured horizontal stress was calculated by dividing the measured force on the block by the area of the block. Values for each variable are reported in table 2, and calculated stresses are reported in table 3.

Table 2. Parameters for the hydrostatic and Jansen pressure equations.

Parameter	Value
Length (L)	0.0762 mm
Gravity acceleration (g)	9.81 m s^{-2}
Height of block (h_3)	0.051 mm
Constant for active stress state (k_A)[a]	0.48
Constant for passive stress state (k_P)[a]	2.07

[a] Calculated using equation 2. The angle of repose (table 1) is assumed equal to the effective angle of internal friction due to the non-cohesive nature of the grain.

Table 3. Calculated values of the hydrostatic, active and passive stresses (kPa).

	Depth (cm)		
Stress	10.2	20.3	30.4
Hydrostatic	0.95	1.71	2.46
Active	0.46	0.82	1.19
Passive	1.96	3.54	5.11

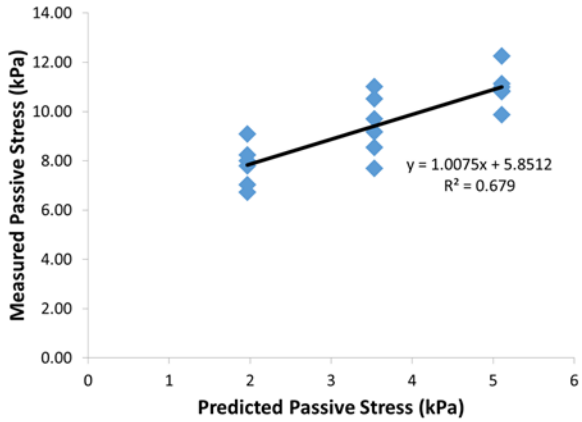

Figure 6. Predicted passive stress plotted against measured passive stress.

Results

Friction Test

The average friction coefficient for steel on steel using the block method was 0.23 (SD 0.03). The friction coefficient measured using the control was 0.22 (SD 0.01). These results are not significantly different from each other ($p = 0.26$) and are within the range of values found in the literature for the kinetic friction coefficient of steel (0.09 to 0.6; Chen, 2004). These results indicate that the virtual work equations developed earlier are a good descriptor for calculating the force acting on the blocks.

Passive Stress Experiment

The passive stress measured by the experiment was 7.82 kPa (SD 0.85 kPa) at 10.2 cm depth, 9.44 kPa (SD 1.24 kPa) at 20.3 cm depth, and 10.98 kPa (SD 0.77 kPa) at 30.4 cm depth. The average relative uncertainty across all replicates was 23.0%, with y accounting for the largest source of uncertainty. These passive stress values were 8.2 times larger than the hydrostatic pressure at 10.2 cm depth, 5.5 times larger than at 20.3 cm depth, and 4.5 times larger than at 30.4 cm depth. In addition, the experimental values were 4.0, 2.7, and 2.2 times larger than predicted passive pressure values at 10.2, 20.3, and 4.5 cm depths, respectively. When the experimentally measured passive stresses were plotted against the predicted passive stresses, and a regression line was fit to the data, the results indicated that experimental results were consistently 5.85 kPa larger regardless of depth (fig. 6).

Discussion

The pressure values measured in this study were larger than expected. Moore and Jones (2017) reported a measured pressure of 2.82 kPa at a corn depth of 23.5 cm in a 1.83 m diameter bin. Similar to this experiment, their stress values was 2 to 5 times larger than stress values from a Janssen analysis assuming an active stress state. In addition, the results in this experiment were 3 to 4 times larger than the pressure values reported by Moore and Jones (2017). This result was expected, as k_P values are about four times larger than k_A values (table 2). Thompson et al. (1997) measured both lateral and vertical stresses and found that the lateral stress was 2.7 times greater than the vertical stress at a grain depth of

2 m in an 11 m diameter bin. One surprising result is that in both this experiment and in the Moore and Jones (2017) study, the measured stress values were 2 to 4 times larger than the values predicted by Janssen's equation.

Study Limitations

One of the most significant limitations of this study was the small size of the tank used in the experiment, which was limited by the dimensions of the Criterion machine. The bin used by Moore and Jones (2017) was 3.5 times the diameter of the tank used in this study (0.41 m vs. 1.83 m). This difference is not expected to affect the conclusions of this study because stress values increase as the hydraulic diameter of a bin increases until it reaches an asymptotic value. In addition, at shallow depths in grain systems, the pressure is approximately hydrostatic and thus independent of the bin diameter. This result was confirmed by Moore and Jones (2017), who found that their pressure values closely mimicked hydrostatic values at shallow depths.

Another concern is the close proximity of the walls and bottom of the bin to the pressure probe, which could have impacted the results. The wooden blocks were approximately 16 cm from the walls and 10 cm from the bottom, and they only moved about 0.5 cm. It is not likely that the walls would have impacted the results, and the results of Thompson et al. (1997) support this conclusion.

Conclusions

The results of this study indicate that the grain pressure on a victim trying to breathe can be 8 to 11 kPa, which is 3 to 4 times larger than the values typically measured with a static load cell. This finding explains the contrast between anecdotal reports of what victims experience and static load cell measurements. This method is a closer approximation to what a victim might experience in a grain entrapment. This result raises concerns because this larger pressure might be enough to inhibit breathing and cause asphyxiation, even if the victim's head is above the grain surface. Hence, expediting the extrication of the victim or removing grain from around the victim with devices such as grain rescue tubes is critical to victim survival under most circumstances. In addition, rescuers should avoid standing on grain on top of or near the victim and should minimize the number of rescuers in the storage facility to limit the amount of pressure that transfers to the victim.

One concern is the variability of the results in this study. We are unsure of why there is a large degree of scatter in the repeat experiments. We were careful to maintain consistency between the repeat experiments and tested potential biases by testing the lubrication before and afterward, conducting studies with settled versus reloaded grain, checking all assumptions in the stress equations, and running an uncertainty analysis. It is not uncommon to see significant variability in repeat experiments involving particulate materials, especially when the particle sizes are of the same order of size as the measurement devices. This variability is due to the statistical variations in the packing of the particles. Because the measurement variability is large, we chose to include all of the data points in the plot so the reader can see the repeat experiment values directly. In addition, similar variability was observed by Moore and Jones (2017).

Future research is needed in full-scale bins to confirm the results of this experiment. This future research could be designed by placing sensors on flat pouches that can be expanded and contracted within the grain to measure potential pressure during inhalation and exhalation.

Acknowledgements

Special thanks to Scott Brand for his help in constructing the box used in these experiments and to Ibrahim Issa for providing the diagrams of the experimental setup (figs. 1 and 2). This research was partially funded by a Purdue Graduate Student Government Research Grant and Purdue's Agricultural Safety and Health Program.

References

ASABE. (2012). S352.2: Moisture measurement—Unground grain and seeds. St. Joseph, MI: ASABE.

Bhadra, R., Casada, M. E., Thompson, S. A., Boac, J. M., Maghirang, R. G., Montross, M. D., ... McNeill, S. G. (2017). Field-observed angles of repose for stored grain in the United States. *Appl. Eng. Agric., 33*(1), 131-137. https://doi.org/10.13031/aea.11894

Chen, E. (2004). Coefficients of friction for steel. In *The physics factbook.* Retrieved from http://hypertextbook.com/facts/2005/steel.shtml

Clementson, C. L., Ileleji, K. E., & Rosentrater, K. A. (2010). Evaluation of measurement procedures used to determine the bulk density of distillers dried grains with solubles (DDGS). *Trans. ASABE, 53*(2), 485-490. https://doi.org/10.13031/2013.29557

Ileleji, K. E., & Zhou, B. (2008). The angle of repose of bulk corn stover particles. *Powder Tech., 187*(2), 110-118. https://doi.org/10.1016/j.powtec.2008.01.029

Issa, S. F. (2016). Exploring the cause of injury or death in grain entrapment, engulfment, and extrication. West Lafayette, IN: Purdue University, Department of Agricultural and Biological Engineering.

Issa, S. F., & Field, W. E. (2017). Determining the pull-forces required to extricate a victim entrapped at various angles in a grain mass. *Safety, 3*(11). https://doi.org/10.3390/safety3010011

Issa, S. F., Cheng, Y. H., & Field, W. (2017a). 2016 summary of U.S. agricultural confined space-related injuries and fatalities. West Lafayette, IN: Purdue University Safety and Health Program.

Issa, S. F., Cheng, Y. H., & Field, W. E. (2016). Summary of agricultural confined-space related cases: 1964-2013. *J. Agric. Saf. Health, 22*(1), 33-45. https://doi.org/10.13031/jash.22.10955

Issa, S. F., Field, W. E., Schwab, C. V., Issa, F. S., & Nauman, E. A. (2017b). Contributing causes of injury or death in grain entrapment, engulfment, and extrication. *J. Agromed., 22*(2), 159-169. https://doi.org/10.1080/1059924X.2017.1283277

Moore, K. G., & Jones, C. L. (2017). Grain entrapment pressure on the torso: Can you breathe while buried in grain? *J. Agric. Saf. Health, 23*(2), 99-107. https://doi.org/10.13031/jash.11648

Nedderman, R. M. (1992). *Statics and kinematics of granular materials.* Cambridge, UK: Cambridge University Press.

Roberts, M., Field, W., Maier, W. E., & Stroshine, R. (2015). Determination of entrapment victim extrication force with and without use of a grain rescue tube. *J. Agric. Saf. Health, 21*(2), 71-83. https://doi.org/10.13031/jash.21.10150

Schmechta, V. H., & Matz, A. (1971). Zum versinken in getreide [About engulfment in grain]. *Zeitschrift für die Gesamte Hygience and Ihre Grenzgebiete, 17*(8), 565-567.

Schwab, C. V., Ross, U. J., Piercy, L. R., & McKenzie, B. A. (1985). Vertical pull and immersion velocity of mannequins trapped in enveloping grain flow. *Trans. ASAE, 28*(6), 1997-2002. https://doi.org/10.13031/2013.32555

Thompson, S. A., Galili, N., & Williams, R. A. (1997). Lateral and vertical pressures in two different full-scale grain bins during loading. *Food Sci. Tech. Intl., 3*(5), 371-379. https://doi.org/10.1177/108201329700300508

Appendix

From the geometry in figure 4b and the Pythagorean theorem:

$$\left(L\sin\theta-\delta y\right)^2+\left(L\cos\theta+\delta x\right)^2=L^2 \tag{16}$$

$$L^2\sin^2\theta-2L\delta y\sin\theta+\left(\delta y\right)^2+L^2\cos^2\theta+2L\delta x\cos\theta+\left(\delta x\right)^2=L^2 \tag{17}$$

$$L^2\underbrace{\left(\sin^2\theta+\cos^2\theta\right)}_{1}-2L\delta y\sin\theta+\underbrace{\left(\delta y\right)^2}_{\text{negligible}}+2L\delta x\cos\theta+\underbrace{\left(\delta x\right)^2}_{\text{negligible}}=L^2 \tag{18}$$

$$\delta x\cos\theta=\delta y\sin\theta \tag{19}$$

$$\delta x=\delta y\tan\theta \tag{5}$$

Note that in going from equation 18 to equation 19, the squares of the virtual displacements have been neglected because these displacements are considered infinitesimally small.

Substituting equation 5 into equation 4 and solving for R gives:

$$0=F\delta y+2W\tfrac{1}{2}\delta y-2\left(R+f\right)\delta y\tan\theta \tag{20}$$

$$R=\frac{F+W}{2\tan\theta}-f \tag{21}$$

or

$$R=\left(F+W\right)\frac{\sqrt{L^2-y^2}}{2y}-f \tag{6}$$

The friction force f is a function of the angle θ or position y, i.e., $f = f(y)$ in general. Hence, at each given position, a different friction force should be used.

Consider the case when the load cell measuring the force F is tared at a given condition. The tared force (F') is then defined as:

$$F'\equiv F-F_{y_0}=F-\left[\frac{2y_0}{\sqrt{L^2-y_0^2}}\left(R_{y_0}+f_{y_0}\right)-W\right] \tag{7}$$

where y_0 is the vertical location at which the load cell is tared. Thus, at position y_0, the tared load cell will register $F' = 0$. The block force R can be found in terms of the tared force by substituting equation 7 into equation 6:

$$R=\left[\left(F'+F_{y_0}\right)+W\right]\frac{\sqrt{L^2-y^2}}{2y}-f \tag{22}$$

By definition, at y_0, $R_{y0} = 0$; thus, using equation 6, F_{y0} can be simplified to:

$$R_{y0} = 0 = \left(F_{y0} + W\right)\frac{\sqrt{L_{y0}^2 - y_{y0}^2}}{2y_0} - f_{y0} \tag{23}$$

$$F_{y0} = \frac{2y_0}{\sqrt{L_{y0}^2 - y_{y0}^2}} f_{y0} - W \tag{24}$$

Substituting F_{y0} into equation 22 yields:

$$R = \left[\left(F' + \left(\frac{2y_0}{\sqrt{L_{y0}^2 - y_{y0}^2}} f_{y0} - W\right)\right) + W\right]\frac{\sqrt{L^2 - y^2}}{2y} - f \tag{25}$$

Simplifying equation 25 yields:

$$R = F'\frac{\sqrt{L^2 - y^2}}{2y} + \left(\frac{2y_0}{\sqrt{L_{y0}^2 - y_{y0}^2}} \times \frac{\sqrt{L^2 - y^2}}{2y}\right) f_{y0} - f \tag{26}$$

Finally, set f' to:

$$f' \equiv f - \left(\frac{2y_0}{\sqrt{L_{y0}^2 - y_{y0}^2}} \times \frac{\sqrt{L^2 - y^2}}{2y}\right) f_{y0} \tag{9}$$

to get:

$$R = F'\frac{\sqrt{L^2 - y^2}}{2y} - f' \tag{8}$$